iScience

CellPress
OPEN ACCESS

Article

Tubule system of earliest shells as a defense against increasing microbial attacks

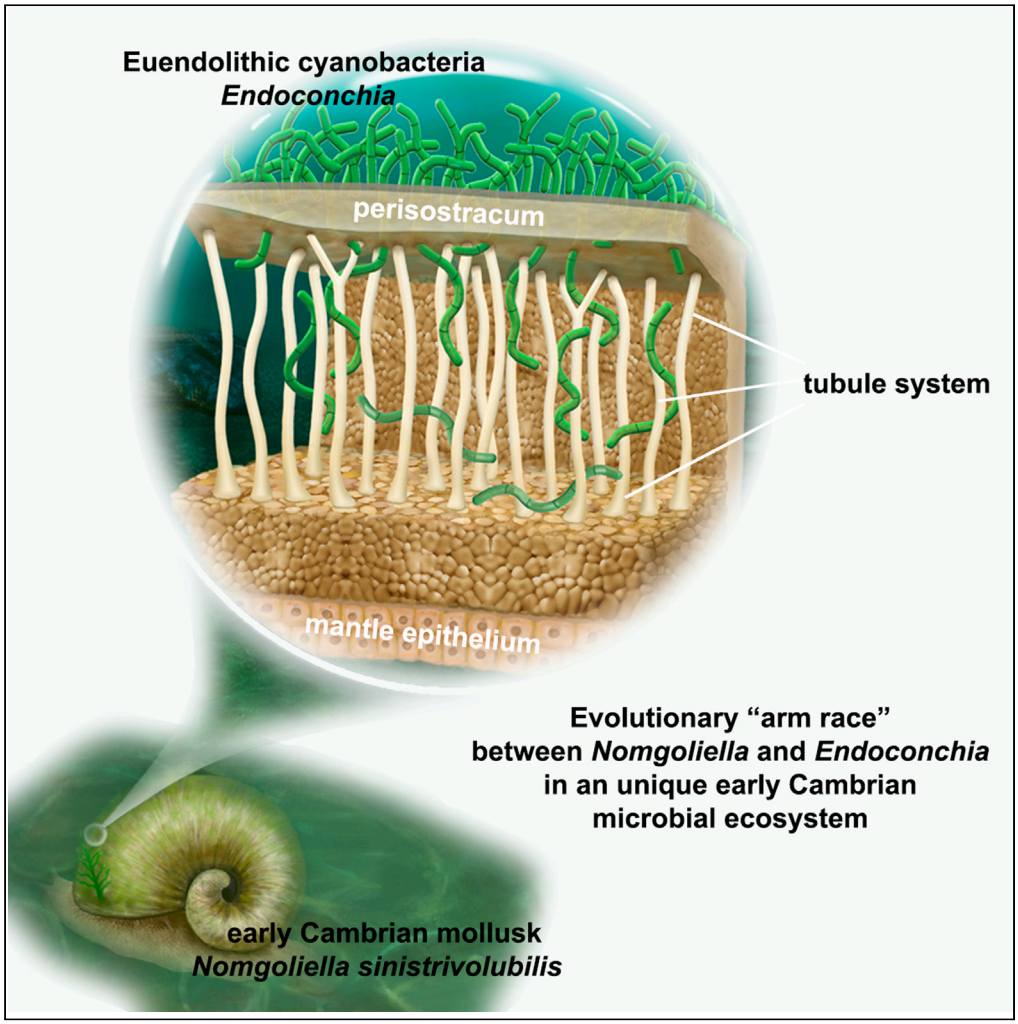

Luoyang Li, Timothy P. Topper, Marissa J. Betts, ..., Christian B. Skovsted, Linhao Cui, Xingliang Zhang

xzhang69@nwu.edu.cn

Highlights

First mineralized mollusks appeared in the early Cambrian microbial ecosystem

Advanced and high density tubule system was discovered in earliest mineralized shells

Shell tubules evolved as a defensive strategy against enhanced microbial attacks

"arm race" between skeletal animals and microorganisms was interpreted as a driving force of evolution

Li et al., iScience 27, 109112
March 15, 2024
https://doi.org/10.1016/j.isci.2024.109112

iScience

CellPress
OPEN ACCESS

Article

Tubule system of earliest shells as a defense against increasing microbial attacks

Luoyang Li,[1,2] Timothy P. Topper,[3,4] Marissa J. Betts,[3,5] Gundsambuu Altanshagai,[6,7] Batktuyag Enkhbaatar,[6] Guoxiang Li,[8] Sanzhong Li,[1,2] Christian B. Skovsted,[4] Linhao Cui,[3,9] and Xingliang Zhang[3,8,10,*]

SUMMARY

The evolutionary mechanism behind the early Cambrian animal skeletonization was a complex and multifaceted process involving environmental, ecological, and biological factors. Predation pressure, oxygenation, and seawater chemistry change have frequently been proposed as the main drivers of this biological innovation, yet the selection pressures from microorganisms have been largely overlooked. Here we present evidence that calcareous shells of the earliest mollusks from the basal Cambrian (Fortunian Age, ca. 539–529 million years ago) of Mongolia developed advanced tubule systems that evolved primarily as a defensive strategy against extensive microbial attacks within a microbe-dominated marine ecosystem. These high-density tubules, comprising approximately 35% of shell volume, enable nascent mineralized mollusks to cope with increasing microbial bioerosion caused by boring endolithic cyanobacteria, and hence represent an innovation in shell calcification. Our finding demonstrates that enhanced microboring pressures played a significant role in shaping the calcification of the earliest mineralized mollusks during the Cambrian Explosion.

INTRODUCTION

The Cambrian Explosion was marked by the abrupt appearances of major animal body plans, including many with biologically controlled mineralized skeletons. This unprecedented evolutionary event in life's history was supposed to be driven by a range of environmental, ecological, and biological factors.[1–5] Ocean oxygenation was widely considered a critical driver,[6–9] enabling the development of complex animal body plans that facilitated the evolution of skeletal structures for support, locomotion, and protection. The rise of predation pressure likely spurred the development of stronger defenses among animals, leading to the emergence of robust exoskeletons.[10–12] Moreover, the excessive concentration of calcium and carbonate ions,[13] mineral constituents of calcareous skeletons, in seawater further stimulated animal skeletonization, as biomineralization probably initiated as a physiological detoxification in response to changing seawater chemistry.[14–16]

Here we present a novel perspective on the driving factors behind the emergence of animal skeletonization during the Ediacaran-Cambrian transition by examining the animal-microbe interactions, specifically the defensive mechanism against microbially induced carbonate erosion (i.e., microbioerosion), by cyanobacterial boring activities (i.e., microborings), and we found the anti-microboring mechanism recorded in shells of earliest Cambrian mollusks from southwestern Mongolia. These earliest calcified mollusk shells exhibited a complex and densely packed canal tubule system, which was utilized to strengthen the shells and defend against co-existing euendolithic cyanobacteria. The presence of such an anti-microboring strategy played a pivotal role in maintaining the structural integrity of shells and facilitating the ecological adaptability of nascent shelled mollusks within contemporaneous microbe-dominated seafloor environments. Hence, the acquisition of intricate tubule systems within shells is interpreted as a result of microboring selection pressure on shell calcification in the earliest mineralized mollusks. These observations provide valuable insights into the interactions between skeletal animals and microborers during the Cambrian Explosion, shedding light on the origin and early diversification of mollusk mineralization, as well as their broader implications for comprehending the complexity of the Earth-Life system in the past and present biosphere.

[1]Frontiers Science Center for Deep Ocean Multispheres and Earth System, Key Lab of Submarine Geosciences and Prospecting Techniques, Ministry of Education and College of Marine Geosciences, Ocean University of China, Qingdao 266100, China
[2]Laboratory for Marine Mineral Resources, National Laboratory for Marine Science and Technology (Qingdao), Qingdao 266237, China
[3]Shaanxi Key Laboratory of Early Life and Environments, State Key Laboratory of Continental Dynamics and Department of Geology, Northwest University, Xi'an 710069, China
[4]Department of Palaeobiology, Swedish Museum of Natural History, Box 50007, 104 05 Stockholm, Sweden
[5]Palaeoscience Research Centre, School of Environmental and Rural Science, University of New England, Armidale, NSW 2351, Australia
[6]Institute of Paleontology, Mongolian Academy of Sciences, Ulaanbaatar 15160, Mongolia
[7]School of Arts and Sciences, National University of Mongolia, Ulaanbaatar 14200, Mongolia
[8]State Key Laboratory of Palaeobiology and Stratigraphy, Nanjing Institute of Geology and Palaeontology, Chinese Academy of Sciences, Nanjing 210008, China
[9]Senior author
[10]Lead contact
*Correspondence: xzhang69@nwu.edu.cn
https://doi.org/10.1016/j.isci.2024.109112

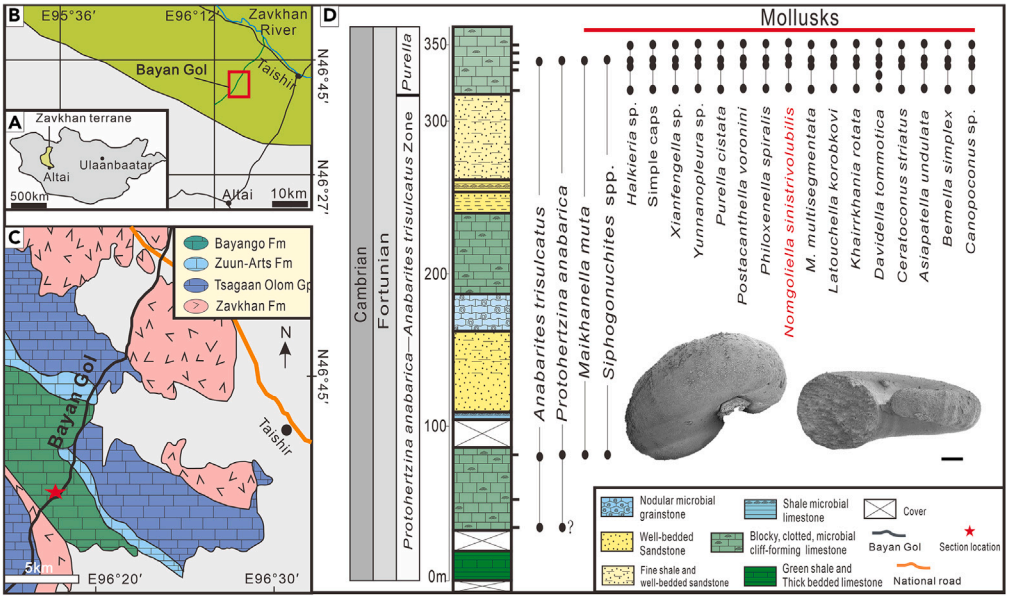

Figure 1. Geological setting and early molluskan diversification in Mongolia

(A) Locality map of the Zavkhan terrane, southwestern Mongolia.

(B) Location of Bayan Gorge in the Zavkhan Basin.

(C) Geological map of Bayan Gorge and the location of the section BAY2, GPS: N46°42′11.0"/E96°18′44.5."

(D) Lithostratigraphic columns of the Bayangol Formation in the BAY2 section and fossil occurrence horizon. The boundary of the small shelly fossil *Protohertzina anabarica-Anabarites trisulcatus* biozone and *Purella* biozone is placed at 335m above the base of the section. Close-up images of sinistrally coiled shells of *Nomgoliella sinistrivolubilis* Missarzhevsky, 1981 showing the preservation of dense shell tubules on the surface of phosphatic internal molds, scale bars: 500 μm; *M. multisegmentata* = *Merismoconcha multisegmentata*.

RESULTS

Geological settings and biostratigraphy of the Bayangol Formation

The Zavkhan terrane is one of the Proterozoic cratonic fragments in southwestern Mongolia that make up the core of the Central Asian orogenic belt.[17] Sedimentary sequences spanning the Ediacaran-Cambrian transition are widespread across the Zavkhan Basin, and in ascending order, comprise the Tsagaan-Olom Group, Zuun-Arts Formation, Bayangol Formation, Salaagol Formation, and Khairkhan Formation.[18] Recent studies developed a comprehensive chronostratigraphic framework, integrating biostratigraphic, lithostratigraphic, and chemostratigraphic data, for the basal Cambrian Zuun-Arts and Bayangol formations (Figures 1A–1C). The Ediacaran-Cambrian boundary was identified at the topmost layer of the Zuun-Arts Formation, marked by a significant negative carbon isotope excursion interpreted as the Basal Cambrian carbon isotope Excursion (BACE).[19] The Bayangol Formation consists of a mixture of carbonate and siliciclastic deposits and contains a diverse range of thrombolites and calcimicrobial reefs, signifying a shallow water carbonate shelf environment dominated by microbial mats.[20,21]

The small shelly fossils in the studied BAY2 section of the Bayangol Formation (coordinates: N46°42′11.0"/E96°18′44.5," true thickness 359m) span two shelly biozones: the *Protohertzina anabarica-Anabarites trisulcatus* Assemblage zone and the *Purella* zone, indicating a Cambrian Fortunian age (ca. 539-529 million years).[22,23] Micromollusks are prominent components of the shelly fossils in this region. The *Protohertzina anabarica-Anabarites trisulcatus* Assemblage zone yields an abundance of scaly cap-shaped maikhanellid shells and siphogonuchitid sclerites, representing stem-group aculiferan mollusks.[24] As we ascend the section, the *Purella* zone witnesses a rapid diversification of micromollusks with coiled, conical, and cyrtoconic shells, representing stem members of conchiferan mollusks.[25] A preliminary investigation of the molluskan assemblage unravels the presence of preserved shell tubules with varying degrees on the surface of phosphatized internal mold specimens across all conchiferan taxa, with *Nomgoliella sinistrivolubilis* Missarzhevsky, 1981 showcasing the best preservation. Shells of *N. sinistrivolubilis* are small, sinistral, and tightly coiled with 1.5 whorls (Figure 1D). Systematic descriptions of this molluskan assemblage will be provided in another article. This study mainly focuses on illustrating the morphology, structure, and function of tubules within *N. sinistrivolubilis* shells, as well as deciphering their ecological importance in the context of an early Cambrian microbial ecosystem.

Preservation and structure of shell tubules

The primary carbonate mineralogy of *N. sinistrivolubilis* shells has been altered during secondary phosphatization and laboratory acid treatment. However, shell tubules (Figure 2A, a diagram illustrating the presence of dense tubules within mineralized shells), which were primarily encased by biogenic minerals in the form of a carbonate sheath, were pseudomorphs in place on the surface of phosphatized internal molds. These tubules are preserved as simple phosphatized columns that connect the internal mold surface to the external phosphatic coatings

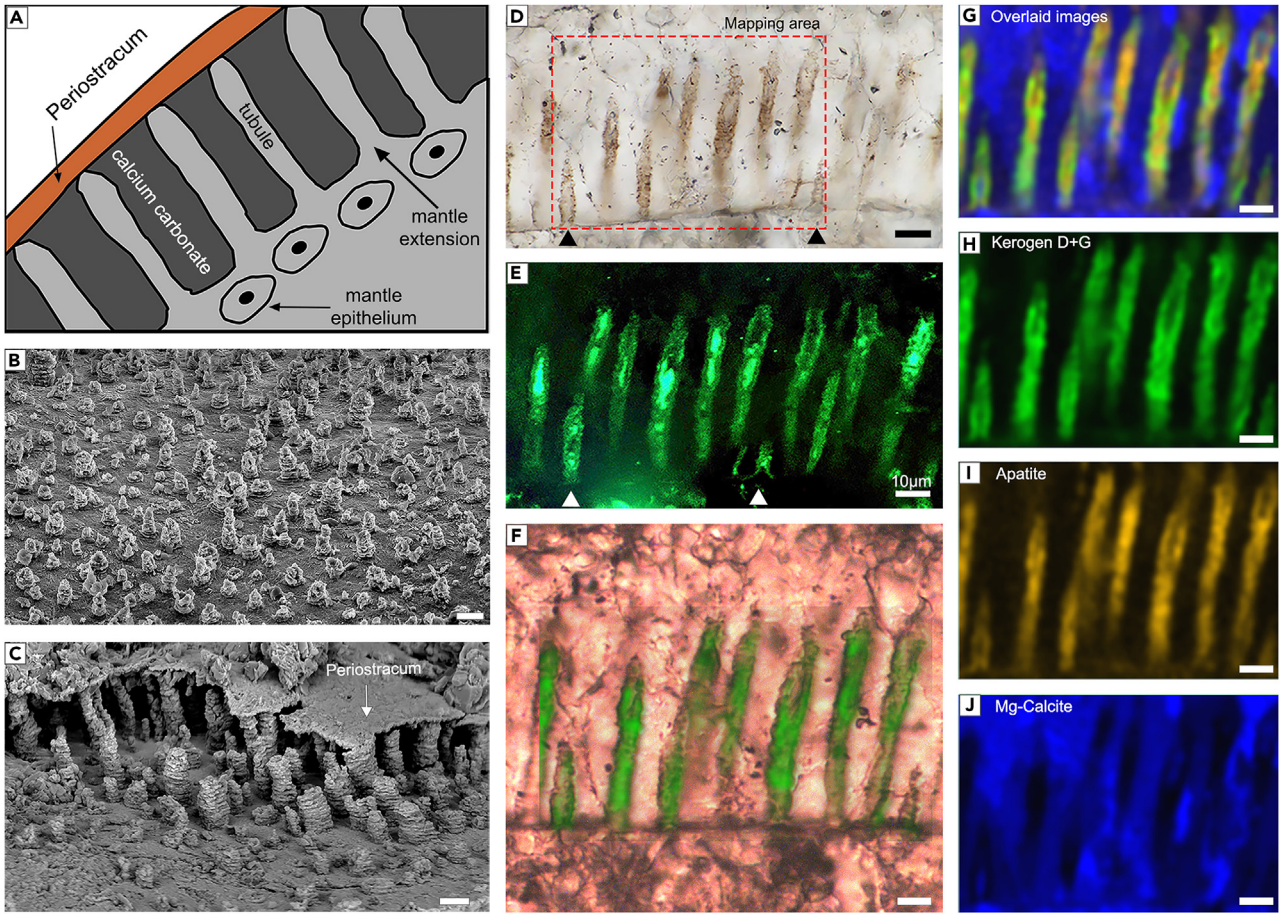

Figure 2. Shell tubule system of *Nomgoliella sinistrivolubilis*

(A) A schematic diagram illustrating the tubules within mineralized shells.

(B) Preservation of dense tubules on internal mold surface (SEM images).

(C) Backscattered electron imaging showing tubules connecting the internal shell surface to the external periostracum.

(D) Optical photomicrographs reveal the round openings on the internal shell surface formed by tubules.

(E) Confocal laser scanning fluorescence imaging shows holes formed by tubules on the shell interior surface, marked with arrowheads.

(F–J) Raman spectroscopic mapping showing the mineral distribution of shells suggest that the tubules consist of apatite and kerogen in contrast to calcite of shell matrix; combined images (F). Scale bars are 10 μm.

(Figure 2C). The external coating represents the replacement of the original organic periostracum by secondary phosphate aggregates during the process of phosphatization. The tubules that originally harbored cellular projections from the mantle form dense round openings on the internal surface of shells (Figure 2D). These shell openings may be infilled secondarily by phosphate minerals, leaving dense tubercles on internal molds (Figure 2B).

The structure of the tubules, characterized by carbonate sheaths and enclosed canals, is best observed on sectioned samples through optical photomicrographs (Figure 2D) and confocal laser scanning microscopy (Figure 2E). Mineralogical analysis using Raman spectroscopic imaging (Figure 2F, combined image) on sectioned samples reveals the presence of organic remnants (kerogens) and apatite minerals in the phosphatized carbonate sheath (Figures 2H and 2I). The mineralogical composition of tubules is in marked contrast to the surrounding shell matrix, which is predominantly composed of calcite after diagenesis (Figures 2G, 2J, and 3). Raman point spectra further corroborate this that the organic remnants of tubules is recognized by two combined intensive bands located at ~1338.3 cm^{-1} and ~ 1610.7 cm^{-1}, abbreviated as "D" (disordered) and "G" (graphitic), respectively. By contrast, the sharp band (Point 2) located at ~1087.7 cm^{-1} indicates a calcitic composition of mineral shells.

Distribution and density of shell tubules

The tubules preserved on the internal molds of the shell are evenly distributed or sometimes aligned in commarginal rows. They are uniformly cylindrical structures that are circular in cross-section and perpendicular to the shell surface. High-resolution scanning electron microscopy and backscattered electron images illustrate discrete ring-like structures of the carbonate sheath (Figures 4A and 4B), indicating the growth stages of the tubule. Bifurcating tubules are occasionally observable (Figures 4C and 4D). Our measurements show that the average diameter

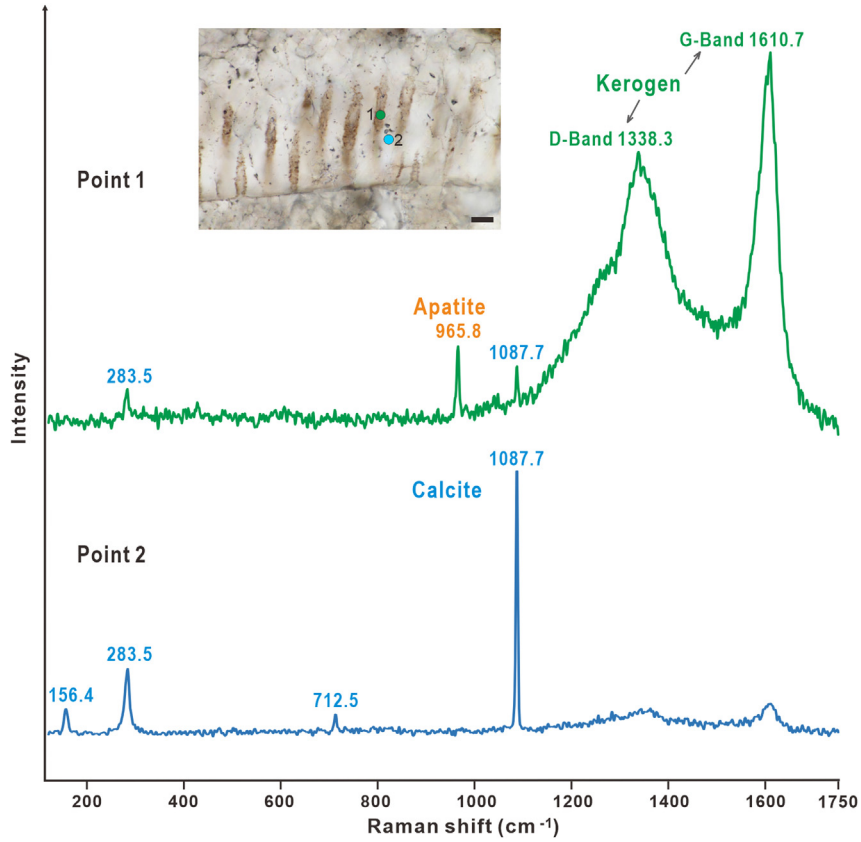

Figure 3. Mineralogical composition of *Nomgoliella sinistrivolubilis* shell

Raman spectra illustrate the carbonaceous kerogen and apatite mineralogy of the shell tubule (point 1) in contrast to the calcite mineralization of the surrounding shell matrix (point 2). Scale bar is 10 μm.

of individual tubules is 6 μm, up to 50 μm in length (= shell thickness), and tubule density ranges from ca. 10,000 to 14,000 per mm^2 (See Table S1). The formation of such a high density tubule system accounts for up to 35% of total shell volume, which requires a large amount of organic content and substantial metabolic energy costs in the process of shell mineralization.

Euendolithic cyanobacterial microborings

Of particular importance is the observation of a specific type of euendolithic cyanobacterial borings formed by *Endoconchia lata* Runnegar, 1985 that co-occurred with tubules on internal molds (Figure 4E). Microborers of this type are widespread in early Cambrian carbonates, most commonly found in mollusks, and are believed to have been formed by euendolithic cyanobacteria.[26,27] Our new observations show that the phosphatic casts of cyanobacterial microborings are filamentous, ca. 6 μm in diameter equivalent to that of shell tubules, ornamented with threaded sculptures that are interpreted as replications of features on the internal surface of microborings (Figure 4I). The *Endoconchia* cast is always parallel or sub-parallel to shell substrates and tends to be surrounding rather than penetrating concerning the tubules and adjacent cyanobacterial microborings (Figures 4F–4H).

DISCUSSION

Prevalence, function, and selective advantage of shell tubules

Specialized cellular extensions, known as caeca, are present in the delicate shell tubules of various mollusk lineages, e.g., extant bivalves, gastropods, polyplacophorans (chitons),[28] and Cambrian helcionelloid mollusks.[29,30] Similar structures, called punctae, are also a characteristic feature of the calcareous skeletons of brachiopods and bryozoans.[31,32] Interestingly, shell tubules in bivalves are formed secondarily through caecal protrusions from the mantle epithelium that dissolve pre-existing shell layers, while the growth of shell tubules in gastropods is more similar to that of brachiopod punctae, which are formed primarily during shell production.[33,34] The structural and growth similarities between shell tubules and punctate are compatible with the notion that shell calcification is an evolutionarily conserved trait shared between mollusks and brachiopods, rooted deeply in their homologous genetic toolkit for biomineralization.[35] In early Cambrian helcionelloid *Nomgoliella* shells, the presence of a thin layer of biogenic carbonate sheath, akin to that of some terebratulide brachiopod punctae,[31]

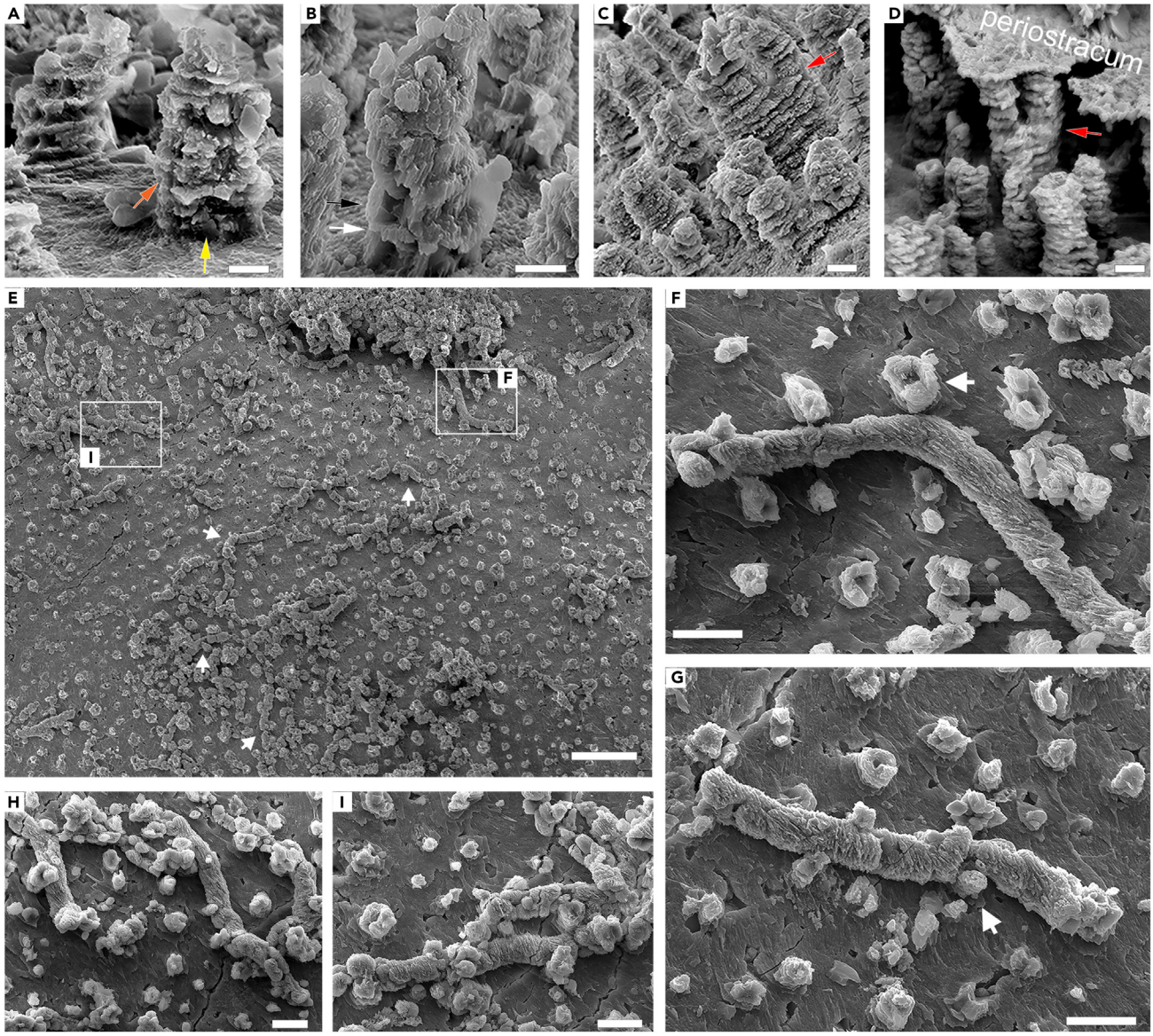

Figure 4. Shell tubule system of *Nomgoliella sinistrivolubilis*

(A–D) Individual tubules consist of an external carbonate sheath and an internal canal.

(A and B) The carbonate sheath of tubules consists of a discrete ring-like structure.

(C and D) Bifurcating tubules, (C) SEM, (D) BSEM photographs.

(E) Overview of shell tubules co-occurring with the cast of euendolithic cyanobacteria.

(F, G, and I) Casts of cyanobacteria filaments ornamented with threaded sculptures are weaved around dense tubules and adjacent cyanobacteria filament (H) on internal mold, (F), inverted images. Scale bars are 2 μm (A, B); 5 μm (C, D); 10 μm (E, G, H, I); 50 μm (E).

demonstrates a primary genesis of tubules in concomitant with the mineralization of the shell. Moreover, the tegmentum layer of chiton shell plates possesses a complex, vertically and horizontally oriented, tissue-filled canal system known as aesthetes. It is well known that aesthetes contain neuronal structures and photoreceptor cells, suggesting a sensory function.[36] The aesthete in chiton differs largely from the morphologically simple and vertically oriented tubules of bivalves, gastropods, and early Cambrian stem-group mollusks.

As a key structure within shells, the tubules/punctae were supposed to serve multiple biological functions, involving respiration, molecular compound synthesis and transport, sensory perception, shell repair, mineralization, protection against boring organisms, and mechanical support.[37] The exact function of tubules has been a long-standing controversy and is still an ongoing debate. Nevertheless, they undoubtedly play a vital role in shell health and ecological adaptability for their hosts, allowing the animal to exploit a wide spectrum of environmental niches. Particularly in shallow marine carbonate environments, there exists a diversity of euendolithic microorganisms (cyanobacteria, fungi,

and algae) that can actively penetrate and chemically etch carbonate skeletons (both living and dead shells).[38,39] Dead shells, lacking biological defenses, are particularly susceptible to microbial attacks.[40,41] Cambrian shelly fossils often experienced extensive perforations by euendolithic cyanobacteria during postmortem burial and fossilization stages,[42,43] which made it difficult to distinguish microbial attacks on either living or dead shells. But given the fact that euendolithic microborers generally indiscriminately invade any abiotic and biotic carbonate substrates and formed microborings are distributed randomly within dead shells, the co-occurrence of some cyanobacterial microborings consistently surrounding the shell tubules in *Nomgoliella* confirms microbial attacks on living shells, and that the tubules themselves perform as obstacles or deterrents against boring microorganisms during the animal's lifetime as believed.[37,44]

In addition, the presence of densely distributed tubules within mineralized exoskeletons can significantly enhance mechanical resistance against physical stress.[45,46] To defend against shell-crushing predators such as sea stars, crabs, and seabirds, modern mollusks have evolved various strategies to strengthen their shells and make them more difficult to break or breach. These defensive adaptations include thick-walled shells, robust external ornaments and complex microstructures that impede crack propagation, and the ability to retract edible tissues deep inside the shell.[10,40] The formation of thick-walled shells and the presence of rigid periostracum outside the mineralized shell layers are particularly effective in countering drilling predation and microborers. Moreover, the organic framework (i.e., organic matrix, accounting for less than 5% of shell weight) within mineralized shells also plays a role in limiting perforation, as some microborers are seemingly unable to penetrate through the intricate organic framework.[47,48]

These defensive adaptations seen in modern shells, however, were largely absent in early Cambrian stem-group members of mollusks. A diverse group of mineralized mollusks that emerged during the Cambrian Terreneuvian have not yet developed heavily calcified shells with prominent ornamentations. Instead, they generally secreted fragile, thin-walled shells with fine ornaments, as seen in *Nomgoliella* herein. Calcareous shells with distinct ornaments in younger taxa, such as the recently discovered helcionelloid *Qingjianlepas* from the 518-million-year-old Qingjiang Biota,[49] occurred approximately 20 million years younger than the first mineralized mollusks found in the Cambrian Fortunian.[29] Additionally, the crystallite organization within shells (i.e., shell microstructure) during the Cambrian Terreneuvian remains primitive with various fibrous, prismatic, and foliated fabrics, indicating a limited level of calcification control.[50,51] By contrast, shell tubules appeared to be more prominent and well-developed in early Cambrian molluskan species than their modern representatives.[30] The high density of tubules may partly serve as a compensation mechanism for the inherent weaknesses of initially mineralized shells, adding complexity to the process of shell calcification in early Cambrian mollusks. Together, the mechanical supports and anti-microboring functions of the tubule system contribute significantly to the structural integrity of shells and the ecological adaptability of skeletonized mollusks in early Cambrian seas.

The impact of animal predation was minimal on early shell evolution

The emergence and progression of life, starting from microbial organisms to complex multicellular beings, were considerably affected by ecological interactions between organisms, primarily, in a broad sense, through predation.[10] The predatory-prey relationship has long been recognized as a decisive selective force driving evolution.[11] In this scenario, biomineralization as a defensive strategy against predation first evolved in protists and basal eukaryotes during the late Neoproterozoic.[52,53] The rise of animal predation during the subsequent Cambrian Explosion further led to the development of complex biomineralized structures in various metazoan clades.[11,54,55] The thickening and increased hardness of mineralized molluskan shells from the early Cambrian onwards reflect a reinforcement of biomineralization mechanisms in response to escalating predation pressures.[56] The remarkable advances in molluskan calcification were manifested by the acquisition of the crossed-lamellar microstructure (the most hierarchically complex and evolutionary successful microstructure in molluskan shells) in the early Cambrian stem-group gastropod *Pelagiella*,[23] and by the exhibition of highly sculptured shells in some helcionelloids during the Cambrian Epoch 2.[49] These adaptations in shell microstructure and morphology coincide with the rise of animal predation and the initial establishment of modern-type animal-dominated marine ecosystems during the period.

Fossil evidence for predation on early skeletal animals of the late Ediacaran and early Cambrian was systematically investigated by Bicknell and Paterson.[57] According to their study, while the oldest instances of predatory boreholes were found in *Cloudina* tubes from the terminal Ediacaran period,[58,59] evidence of predation in early Cambrian small shelly fossils is rare. In particular, the development of hard parts in mollusks has traditionally been believed to be protective armour against predators capable of crushing their shells, yet there is a lack of conclusive evidence of predators targeting molluskan prey during the Cambrian Terreneuvian Epoch.[57] Fossil evidence of drilling and puncture marks became more common in Cambrian Miaolingian and Furongian skeletal taxa, but primarily on brachiopod shells. The reasons why brachiopod shells were preferentially preyed upon by drilling and durophagous predators remain unclear, but it is likely due to the higher organic content of their organophosphate shells. Furthermore, it has been proposed that some Cambrian euarthropods with gnathobase appendages may have been potential predators of shelled mollusks, but undisputed arthropod body fossils did not appear until the Cambrian Series 2.[60] A recent interesting study further suggested that radiodont euarthropods (despite being a raptorial predator of the Cambrian communities) were seemingly incapable of crushing biomineralized prey using their spinose frontal appendages.[61] These observations suggest that the impact of animal predation on the evolution of shell-bearing mollusks may have been minimal during the initial diversification of molluskan shell biomineralization in the Cambrian Terreneuvian, though predation pressure was most frequently discussed as a driving force for biomineralization.

Shell tubules evolved in response to increasing microbial attack

The origin and diversification of skeletonized animals took place within a world dominated by microbes. During the terminal Ediacaran, weakly calcified or organic-walled tubular forms, e.g., *Cloudina*, emerged in carbonate environments with the seafloor covered with microbial

Figure 5. An artist reconstruction of *Nomgoliella sinistrivolubilis* in early Cambrian microbial ecosystem

mats.[62–64] These unique Ediacaran-type microbial ecosystems persisted into the earliest Cambrian (Terreneuvian),[65,66] and boosted the development of complex and highly calcified skeletons in bilaterians, contributing to the vast biodiversity of the Cambrian marine communities. The close interactions between early animals and microorganisms seem to confer significant evolutionary and ecological benefits, improving resistance to environmental stress and facilitating the process of forming intricate calcified structures.[67,68] The widespread presence of seafloor microbial mats created a favoring habitat not only for non-skeletal Ediacaran organisms but also for subsequent skeletonized animals by forming nutrient-rich, oxygenated, and carbonate-saturated conditions necessary for the costly biomineralization processes of early marine biocalcifiers.[69]

Importantly but largely overlooked, unconstrained flourishing and rampant growth of microalgae and cyanobacteria, similar to present-day microbial blooms, may impose significant challenges to the health of ecosystems and animals in the context of early Cambrian greenhouse environments.[70,71] This is manifested in the calcareous skeletons of *Anabarites* from the Cambrian Fortunian, which were heavily infested and overwhelmingly penetrated by euendolithic microorganisms, including *Endoconchia* when exposed to seafloor microbial "mat-grounds".[42] Skeletal carbonate was invaded soon after the evolution of mineralized skeletons, and they appeared to be more heavily attacked in productive water than elsewhere.[72,73] The flourishing of euendolithic cyanobacteria and algae may have exerted substantial influence, far surpassing the impact of metazoan predation on the early evolution of molluskan shell calcification in the context of the microbe-dominated ecosystems of the late Ediacaran and earliest Cambrian (Terreneuvian).

During the Ediacaran-Cambrian transition, the remarkable perturbation of Earth's environments, especially the increasing temperatures and high concentration of calcium and carbonate ions in seawater was perceived to have stimulated the widespread calcification of cyanobacterial sheaths.[74] In comparison with the biologically controlled mineralization of complex metazoans, the hyper-calcifying algae and cyanobacteria (i.e., biologically induced mineralization) were more susceptible to changing seawater chemistry due to their weak controls over calcification processes.[75] As a result, a boring lifestyle was widely acquired by hyper-calcifying microorganisms, which was considered to serve as a demineralization strategy escaping from over-calcification.[76] Additionally, the apparent decline of microbial mats induced by the rise of grazing mollusks and burrowing animals may have prompted another selection pressure that encouraged a boring mode of life. Conversely, the increasing penetrating ability of euendoliths and their bloom on shallow-water carbonate settings[27,42,73] imposed substantial risks to skeletonized animals exposed to them, hence exerting strong selection pressure. Finally, the microbial selection pressure impacted shell calcification, which further resulted in the evolution of a much more pronounced and high-density tubule system within molluskan shells.

This complex interaction between skeletonized animals and euendoliths set the biological "arms race" that drove the early evolution of animal skeletal biomineralization during the Cambrian Explosion (Figure 5).

Overall, our study provides new insights into the evolutionary mechanisms underlying the widespread appearance of skeletonized animals during the period of the Cambrian explosion. The advent of mineralized skeletons within a clade in the late Ediacaran and early Cambrian was not only driven by environmental and macro-biotic changes but also substantially influenced by the presence of microboring pressure in the context of the microbe-dominated marine ecosystem. The initially skeletonized molluskan taxa in the Cambrian Terreneuvian evolved well-developed and high-density tubule systems within their shells as a defensive strategy against increasing microborings caused by the rise of euendolithic microorganisms. The development of an anti-microboring mechanism (i.e., tubules) and its prevalence in early molluskan shells enabled nascent mineralized mollusks to survive and exploit the seafloor microbial mat environments, which further contributed to the reform of seafloor substrates from microbe-to animal dominated types, a substrate revolution that profoundly changed the biosphere.

Limitations of the study

Although the acquisition of a pore-tubule system within mollusk shells is an important defensive strategy against increasing microbioerosion, it remains difficult to precisely assess the impact of microbial selection pressure on the evolution of mollusk mineralization solely based on shell characteristics. To support our hypothesis and further understand the rise of mineralized animals in the earliest Cambrian microbial ecosystem, future studies could consider investigating the ecological interaction between microorganisms and other skeletal animals such as hyoliths and brachiopods to gain a deeper understanding of the Cambrian animal skeletonization and the animal-microbe interactions during the Cambrian Explosion.

STAR★METHODS

Detailed methods are provided in the online version of this paper and include the following:

- KEY RESOURCES TABLE
- RESOURCE AVAILABILITY
  - Lead contact
  - Materials availability
  - Data and code availability
- EXPERIMENTAL MODEL AND STUDY PARTICIPANT DETAILS
- METHOD DETAILS
  - Material and sample preparation
  - Electron microscopy
  - Optical microscopy
  - Confocal laser scanning microscopy
  - Raman spectroscopy
- QUANTIFICATION AND STATISTICAL ANALYSIS

SUPPLEMENTAL INFORMATION

Supplemental information can be found online at https://doi.org/10.1016/j.isci.2024.109112.

ACKNOWLEDGMENTS

This study was funded by the National Natural Science Foundation of China (grants 41930319, 41890845, 42121005, 41890844, 42202001, and 42072003); the China Postdoctoral Science Foundation (grant 2022M712987); and the Swedish Research Council (grants VR2016-04610, VR2017-05183, and VR2021-04295). Thanks to our field chef Usukhbayar and our Mongolian drivers Batsaikhan, Todbayar, Batshatar, Bayarsaikhan, and Batkhuyag. We thank Baige Xia at the Northwest University (NWU) and Chunmei Xin at the Ocean University of China (OUC) for technique assistance, and Hao Yun at the NWU and Bing Pan at the Nanjing Institute of Geology and Palaeontology, Chinese Academy of Sciences (NIGPAS) for valuable discussion on the initial draft of the article. Special thanks were given to the Editor Ryan Perry and anonymous reviewers for their constructive comments and suggestions.

AUTHOR CONTRIBUTIONS

Conceptualization, L.Y.L. and L.H.C.; methodology, L.Y.L. and L.H.C.; investigation, L.Y.L., L.H.C., and X.L.Z.; writing – original draft, L.Y.L.; writing – review and editing, L.Y.L., L.H.C., X.L.Z., T.P.T., M.J.B, G.X.L.,and S.Z.L.; funding acquisition, C.B.S., L.Y.L., and X.L.Z.; resources, L.Y.L., G.A., and B.E.; supervision, X.L.Z.

DECLARATION OF INTERESTS

The authors declare no competing interests.

Received: September 23, 2023
Revised: November 14, 2023
Accepted: January 31, 2024
Published: February 6, 2024

REFERENCES

1. Erwin, D.H., Laflamme, M., Tweedt, S.M., Sperling, E.A., Pisani, D., and Peterson, K.J. (2011). The Cambrian conundrum: early divergence and later ecological success in the early history of animals. Science *334*, 1091–1097. https://doi.org/10.1126/science.1206375.
2. Smith, M.P., and Harper, D.A.T. (2013). Causes of the Cambrian explosion. Science *341*, 1355–1356. https://doi.org/10.1126/science.1239450.
3. Zhang, X., Shu, D., Han, J., Zhang, Z., Liu, J., and Fu, D. (2014). Triggers for the Cambrian explosion: hypotheses and problems. Gondwana Res. *25*, 896–909. https://doi.org/10.1016/j.gr.2013.06.001.
4. Briggs, D.E.G. (2015). The cambrian explosion. Curr. Biol. *25*, 864–868. https://doi.org/10.1016/j.cub.2015.04.047.
5. Budd, G.E., and Jackson, I.S.C. (2016). Ecological innovations in the Cambrian and the origins of the crown group phyla. Philos. Trans. R. Soc. Lond. B Biol. Sci. *371*, 20150287. https://doi.org/10.1098/rstb.2015.0287.
6. Sperling, E.A., Frieder, C.A., Raman, A.V., Girguis, P.R., Levin, L.A., and Knoll, A.H. (2013). Oxygen, ecology, and the Cambrian radiation of animals. Proc. Natl. Acad. Sci. USA *110*, 13446–13451. https://doi.org/10.1073/pnas.1312778110.
7. Zhang, X., and Cui, L. (2016). Oxygen requirements for the Cambrian explosion. J. Earth Sci. *27*, 187–195. https://doi.org/10.1007/s12583-016-0690-8.
8. Wood, R., Ivantsov, A.Y., and Zhuravlev, A.Y. (2017). First macrobiota biomineralization was environmentally triggered. Proc. Biol. Sci. *284*, 20170059. https://doi.org/10.1098/rspb.2017.0059.
9. He, T., Zhu, M., Mills, B.J.W., Wynn, P.M., Zhuravlev, A.Y., Tostevin, R., Pogge von Strandmann, P.A.E., Yang, A., Poulton, S.W., and Shields, G.A. (2019). Possible links between extreme oxygen perturbations and the Cambrian radiation of animals. Nat. Geosci. *12*, 468–474. https://doi.org/10.1038/s41561-019-0357-z.
10. Vermeij, G.J. (1989). The origin of skeletons. Palaios *4*, 585–589. https://doi.org/10.2307/3514748.
11. Bengtson, S. (2002). Origins and early evolution of predation. Paleontol. Soc. Pap. *8*, 289–318. https://doi.org/10.1017/s1089332600001133.
12. Wood, R., and Zhuravlev, A.Y. (2012). Escalation and ecological selectively of mineralogy in the Cambrian Radiation of skeletons. Earth Sci. Rev. *115*, 249–261. https://doi.org/10.1016/j.earscirev.2012.10.002.
13. Peters, S.E., and Gaines, R.R. (2012). Formation of the 'Great Unconformity'as a trigger for the Cambrian explosion. Nature *484*, 363–366. https://doi.org/10.1038/nature10969.
14. Simkiss, K. (1977). Biomineralization and detoxification. Calcif. Tissue Res. *24*, 199–200. https://doi.org/10.1007/BF02223316.
15. Degens, E.T., Kazmierczak, J.O.Z.E.F., and Ittekkot, V. (1985). Cellular response to Ca^{2+} stress and its geological implications. Acta Palaeontol. Pol. *30*, 115–135.
16. Wood, R.A. (2011). Paleoecology of the earliest skeletal metazoan communities: implications for early biomineralization. Earth Sci. Rev. *106*, 184–190. https://doi.org/10.1016/j.earscirev.2011.01.011.
17. Steiner, M., Hohl, S.V., Yang, B., Huang, X., and Li, D. (2021). Rewriting the Cambrian biogeography of the Central Asian Orogenic Belt using combined faunal cluster, zircon age and C isotope analysis. Geophys. Res. Lett. *48*, e2021GL093133. https://doi.org/10.1029/2021GL093133.
18. Smith, E.F., Macdonald, F.A., Petach, T.A., Bold, U., and Schrag, D.P. (2016). Integrated stratigraphic, geochemical, and paleontological late Ediacaran to early Cambrian records from southwestern Mongolia. Bulletin *128*, 442–468. https://doi.org/10.1130/b31248.1.
19. Topper, T., Betts, M.J., Dorjnamjaa, D., Li, G., Li, L., Altanshagai, G., Enkhbaatar, B., and Skovsted, C.B. (2022). Locating the BACE of the Cambrian: Bayan Gol in southwestern Mongolia and global correlation of the Ediacaran–Cambrian boundary. Earth Sci. Rev. *229*, 104017. https://doi.org/10.1016/j.earscirev.2022.104017.
20. Wood, R., Zhuravlev, A.Y., and Anaaz, C.T. (1993). The ecology of Lower Cambrian buildups from Zuune Arts, Mongolia: implications for early metazoan reef evolution. Sedimentology *40*, 829–858. https://doi.org/10.1111/j.1365-3091.1993.tb01364.x.
21. Adachi, N., Ezaki, Y., Liu, J., Watabe, M., Altanshagai, G., Enkhbaatar, B., and Dorjnamjaa, D. (2021). Earliest known Cambrian calcimicrobial reefs occur in the Gobi-Altai, western Mongolia: Intriguing geobiological products immediately after the Ediacaran–Cambrian boundary. Global Planet. Change *203*, 103530. https://doi.org/10.1016/j.gloplacha.2021.103530.
22. Brasier, M.D., Shields, G., Kuleshov, V.N., and Zhegallo, E.A. (1996). Integrated chemo-and biostratigraphic calibration of early animal evolution: Neoproterozoic–early Cambrian of southwest Mongolia. Geol. Mag. *133*, 445–485. https://doi.org/10.1017/s0016756800007603.
23. Li, L., Topper, T.P., Betts, M.J., Dorjnamjaa, D., Altanshagai, G., Enkhbaatar, B., Li, G., and Skovsted, C.B. (2023). Calcitic shells in the aragonite sea of the earliest Cambrian. Geology *51*, 8–12. https://doi.org/10.3390/biology12010113.
24. Vinther, J., Sperling, E.A., Briggs, D.E.G., and Peterson, K.J. (2012). A molecular palaeobiological hypothesis for the origin of aplacophoran molluscs and their derivation from chiton-like ancestors. Proc. Biol. Sci. *279*, 1259–1268. https://doi.org/10.1098/rspb.2011.1773.
25. Thomas, R.D.K., Runnegar, B., and Matt, K. (2020). Pelagiella exigua, an early Cambrian stem gastropod with chaetae: lophotrochozoan heritage and conchiferan novelty. Palaeontology *63*, 601–627. https://doi.org/10.1111/pala.12476.
26. Runnegar, B. (1985). Early Cambrian endolithic algae. Alcheringa *9*, 179–182. https://doi.org/10.1080/03115518508618966.
27. Bengtson, S., Conway Morris, S., Cooper, B.J., Jell, P.A., and Runnegar, B.N. (1990). Early Cambrian fossils from South Australia. Australas. Assoc. Palaeontol. Mem. *9*, 232–256.
28. Malchus, N. (2010). Shell tubules in condylocardiinae (Bivalvia: Carditoidea). J. Molluscan Stud. *76*, 401–403. https://doi.org/10.1093/mollus/eyq030.
29. Kouchinsky, A. (2000). Shell microstructures in Early Cambrian molluscs. Acta Palaeontol. Pol. *45*, 119–150.
30. Parkhaev, P.Y. (2006). On the genus *Auricullina* Vassiljeva, 1998 and shell pores of the Cambrian helcionelloid mollusks. Paleontol. J. *40*, 20–33. https://doi.org/10.1134/s0031030106010035.
31. Pérez-Huerta, A., Cusack, M., McDonald, S., Marone, F., Stampanoni, M., and Mackay, S. (2009). Brachiopod punctae: a complexity in shell biomineralisation. J. Struct. Biol. *167*, 62–67. https://doi.org/10.1016/j.jsb.2009.03.013.
32. Taylor, P.D., Vinn, O., and Wilson, M.A. (2010). Evolution of biomineralization in 'Lophophorates'. Spec. Pap. Palaeontol. *84*, 317–333. https://doi.org/10.1111/j.1475-4983.2010.00985.x.
33. Tan-Tiu, A. (1989). Shell tubules in Corbicula fluminea (Bivalvia: Heterodonta): Functional morphology and microstructure. Nautilus *103*, 36–39.
34. Reindl, S., and Haszprunar, G. (1994). Light and electron microscopical investigations on shell pores (caeca) of fissurellid limpets (Mollusca: Archaeogastropoda). J. Zool. *233*, 385–404. https://doi.org/10.1111/j.1469-7998.1994.tb05272.x.
35. Wernström, J.V., Gąsiorowski, L., and Hejnol, A. (2022). Brachiopod and mollusc biomineralisation is a conserved process that was lost in the phoronid–bryozoan stem lineage. EvoDevo *13*, 17. https://doi.org/10.1186/s13227-022-00202-8.
36. Vendrasco, M.J., Fernandez, C.Z., Eernisse, D.J., and Runnegar, B. (2008). Aesthete canal morphology in the Mopaliidae (Polyplacophora). Am. Malacol. Bull. *25*, 51–69. https://doi.org/10.4003/0740-2783-25.1.51.
37. Reindl, S., and Haszprunar, G. (1996). Fine structure of caeca and mantle of arcoid and limopsoid bivalves (Mollusca: Pteriomorpha). Veliger *39*, 101–116.
38. Golubic, S., Radtke, G., and Le Campion-Alsumard, T. (2005). Endolithic fungi in marine ecosystems. Trends Microbiol. *13*, 229–235. https://doi.org/10.1016/j.tim.2005.03.007.
39. Radtke, G., and Golubic, S. (2005). Microborings in mollusk shells, Bay of Safaga, Egypt: Morphometry and ichnology. Facies

51, 118–134. https://doi.org/10.1007/s10347-005-0016-02.
40. Pantazidou, A., Louvrou, I., and Economou-Amilli, A. (2006). Euendolithic shell-boring cyanobacteria and chlorophytes from the saline lagoon Ahivadolimni on Milos Island, Greece. Eur. J. Phycol. *41*, 189–200. https://doi.org/10.1080/09670260600649420.
41. Delvene, G., Lozano, R.P., Piñuela, L., Mediavilla, R., and García-Ramos, J.C. (2022). Autofluorescence of microborings in fossil freshwater bivalve shells. Lethaia *55*, 1–12. https://doi.org/10.18261/let.55.4.7.
42. Stockfors, M., and Peel, J.S. (2005). Euendoliths and cryptoendoliths within late Middle Cambrian brachiopod shells from North Greenland. GFF *127*, 187–194. https://doi.org/10.1080/11035890501273187.
43. Yang, X.G., Han, J., Wang, X., Schiffbauer, J.D., Uesugi, K., Sasaki, O., and Komiya, T. (2017). Euendoliths versus ambient inclusion trails from early Cambrian Kuanchuanpu Formation, South China. Palaeogeogr. Palaeocl. *476*, 147–157. https://doi.org/10.1016/j.palaeo.2017.03.028.
44. Curry, G.B. (1983). Microborings in Recent brachiopods and the functions of caeca. Lethaia *16*, 119–127. https://doi.org/10.1111/j.1502-3931.1983.tb01707.x.
45. Chen, P.Y., Lin, A.Y.M., McKittrick, J., and Meyers, M.A. (2008). Structure and mechanical properties of crab exoskeletons. Acta Biomater. *4*, 587–596. https://doi.org/10.1016/j.actbio.2007.12.010.
46. Tian, X., Han, Z., Li, X., Pu, Z., and Ren, L. (2010). Biological coupling anti-wear properties of three typical molluscan shells—*Scapharca subcrenata, Rapana venosa* and *Acanthochiton rubrolineatus*. Sci. China Technol. Sci. *53*, 2905–2913. https://doi.org/10.1007/s11431-010-4131-0.
47. Golubic, S., Perkins, R.D., and Lukas, K.J. (1975). Boring microorganisms and microborings in carbonate substrates. In The Study of Trace Fossils: A Synthesis of Principles, Problems, and Procedures in Ichnology, R.W. Frey, ed. (Springer Berlin Heidelberg), pp. 229–259.
48. Tribollet, A., and Payri, C. (2001). Bioerosion of the coralline alga Hydrolithon onkodes by microborers in the coral reefs of Moorea, French Polynesia. Oceanol. Acta *24*, 329–342. https://doi.org/10.1016/s0399-1784(01)01150-1.
49. Li, L., Skovsted, C.B., Dai, T., Yun, H., Fu, D., and Zhang, X. (2021). Qingjianglepas from the Qingjiang biota, an evolutionary dead-end of Cambrian helcionelloid mollusks? Palaeogeogr. Palaeocl. *575*, 110480. https://doi.org/10.1016/j.palaeo.2021.110480.
50. Vendrasco, M.J., Rodríguez-Navarro, A.B., Checa, A.G., Devaere, L., and Porter, S.M. (2016). To infer the early evolution of mollusc shell microstructures. Key Eng. Mater. *672*, 113–133. https://doi.org/10.4028/www.scientific.net/kem.672.1.
51. Li, L., Zhang, X., Yun, H., and Li, G. (2017). Complex hierarchical microstructures of Cambrian mollusk Pelagiella: insight into early biomineralization and evolution. Sci. Rep. *7*, 1935. https://doi.org/10.1038/s41598-017-02235-9.
52. Porter, S.M. (2016). Tiny vampires in ancient seas: evidence for predation via perforation in fossils from the 780–740 million-year-old Chuar Group, Grand Canyon, USA. Proc. Biol. Sci. *283*, 20160221. https://doi.org/10.1098/rspb.2016.0221.
53. Cohen, P.A., and Riedman, L.A. (2018). It's a protist-eat-protist world: recalcitrance, predation, and evolution in the Tonian–Cryogenian ocean. Emerg. Top. Life Sci. *2*, 173–180. https://doi.org/10.1042/ETLS20170145.
54. Porter, S. (2011). The rise of predators. Geology *39*, 607–608. https://doi.org/10.1130/focus062011.1.
55. Vinn, O. (2018). Traces of predation in the Cambrian. Hist. Biol. *30*, 1043–1049. https://doi.org/10.1080/08912963.2017.1329305.
56. Vendrasco, M.J., Checa, A.G., and Kouchinsky, A.V. (2011). Shell microstructure of the early bivalve Pojetaia and the independent origin of nacre within the Mollusca. Palaeontology *54*, 825–850. https://doi.org/10.1111/j.1475-4983.2011.01056.x.
57. Bicknell, R.D.C., and Paterson, J.R. (2018). Reappraising the early evidence of durophagy and drilling predation in the fossil record: implications for escalation and the Cambrian Explosion. Biol. Rev. Camb. Phil. Soc. *93*, 754–784. https://doi.org/10.1111/brv.12365.
58. Bengtson, S., and Zhao, Y. (1992). Predatorial borings in late Precambrian mineralized exoskeletons. Science *257*, 367–369. https://doi.org/10.1126/science.257.5068.367.
59. Hua, H., Pratt, B.R., and Zhang, L.Y. (2003). Borings in Cloudina shells: complex predator-prey dynamics in the terminal Neoproterozoic. Palaios *18*, 454–459. https://doi.org/10.1669/0883-1351(2003)018<0454:BICSCP>2.0.CO;2.
60. Zhang, X., Ahlberg, P., Babcock, L.E., Choi, D.K., Geyer, G., Gozalo, R., Stewart Hollingsworth, J., Li, G., Naimark, E.B., Pegel, T., et al. (2017). Challenges in defining the base of Cambrian Series 2 and Stage 3. Earth Sci. Rev. *172*, 124–139. https://doi.org/10.1016/j.earscirev.2017.07.017.
61. Bicknell, R.D.C., Schmidt, M., Rahman, I.A., Edgecombe, G.D., Gutarra, S., Daley, A.C., Melzer, R.R., Wroe, S., and Paterson, J.R. (2023). Raptorial appendages of the Cambrian apex predator Anomalocaris canadensis are built for soft prey and speed. Proc. Biol. Sci. *290*, 20230638. https://doi.org/10.1098/rspb.2023.0638.
62. Hua, H., Chen, Z., Yuan, X., Zhang, L., and Xiao, S. (2005). Skeletogenesis and asexual reproduction in the earliest biomineralizing animal Cloudina. Geol. *33*, 277–280. https://doi.org/10.1130/g21198.1.
63. Shore, A., Wood, R., Curtis, A., and Bowyer, F. (2020). Multiple branching and attachment structures in cloudinomorphs, Nama Group, Namibia. Geology *48*, 877–881. https://doi.org/10.1130/g47447.1.
64. Yang, B., Warren, L.V., Steiner, M., Smith, E.F., and Liu, P. (2022). Taxonomic revision of Ediacaran tubular fossils: Cloudina, Sinotubulites and Conotubus. J. Paleontol. *96*, 256–273. https://doi.org/10.1017/jpa.2021.95.
65. Buatois, L.A., Narbonne, G.M., Mángano, M.G., Carmona, N.B., and Myrow, P. (2014). Ediacaran matground ecology persisted into the earliest Cambrian. Nat. Commun. *5*, 3544. https://doi.org/10.1038/ncomms4544.
66. Tarhan, L.G., Droser, M.L., Planavsky, N.J., and Johnston, D.T. (2015). Protracted development of bioturbation through the early Palaeozoic Era. Nat. Geosci. *8*, 865–869. https://doi.org/10.1038/ngeo2537.
67. Wood, R. (2018). Exploring the drivers of early biomineralization. Emerg. Top. Life Sci. *2*, 201–212. https://doi.org/10.1042/ETLS20170164.
68. Curtis, A., Wood, R., Bowyer, F., Shore, A., Curtis-Walcott, A., and Robertsson, J. (2021). Modelling Ediacaran metazoan–microbial reef growth. Sedimentology *68*, 1877–1892. https://doi.org/10.1111/sed.12832.
69. Becker-Kerber, B., Pacheco, M.L.A.F., Rudnitzki, I.D., Galante, D., Rodrigues, F., and Leme, J.D.M. (2017). Ecological interactions in Cloudina from the Ediacaran of Brazil: implications for the rise of animal biomineralization. Sci. Rep. *7*, 5482. https://doi.org/10.1038/s41598-017-05753-8.
70. Hearing, T.W., Harvey, T.H.P., Williams, M., Leng, M.J., Lamb, A.L., Wilby, P.R., Gabbott, S.E., Pohl, A., and Donnadieu, Y. (2018). An early Cambrian greenhouse climate. Sci. Adv. *4*, eaar5690. https://doi.org/10.1126/sciadv.aar5690.
71. Liu, W., Chang, C., Yun, H., Cui, L., and Zhang, X. (2021). A laminated microbial ecosystem at the summit of the Cambrian Explosion. Global Planet. Change *205*, 103619. https://doi.org/10.1016/j.gloplacha.2021.103619.
72. Lescinsky, H.L., Edinger, E., and Risk, M.J. (2002). Mollusc shell encrustation and bioerosion rates in a modern epeiric sea: taphonomy experiments in the Java Sea, Indonesia. Palaios *17*, 171–191. https://doi.org/10.1669/0883-1351(2002)017<0171:mseabr>2.0.co;2.
73. Cui, L., Liu, W., and Zhang, X. (2020). Phosphatized microbial fossils from the lowest Cambrian of South China and their ecological and environmental implications for the Kuanchuanpu biota. Precambrian Res. *338*, 105560. https://doi.org/10.1016/j.precamres.2019.105560.
74. Riding, R. (2006). Cyanobacterial calcification, carbon dioxide concentrating mechanisms, and Proterozoic–Cambrian changes in atmospheric composition. Geobiology *4*, 299–316. https://doi.org/10.1111/j.1472-4669.2006.00087.x.
75. Ries, J.B. (2010). Review: Geological and experimental evidence for secular variation in seawater Mg/Ca (calcite-aragonite seas) and its effects on marine biological calcification. Biogeosciences *7*, 2795–2849. https://doi.org/10.5194/bg-7-2795-2010.
76. Cockell, C.S., and Herrera, A. (2008). Why are some microorganisms boring? Trends Microbiol. *16*, 101–106. https://doi.org/10.1016/j.tim.2007.12.007.
77. Bouton, G.D. (2008). CorelDRAW: The Official Guide (Mcgraw-hill Osborne). 9780071545709.
78. Press, A. (2010). Adobe Photoshop CS5 - Classroom in a Book, *34*, pp. 336–352. https://doi.org/10.3109/17453054.2011.604842.
79. Burger, W., and Burge, M.J. (2006). ImageJ (Springer Berlin Heidelberg). https://doi.org/10.1007/3-540-30941-1_3.

STAR★METHODS

KEY RESOURCES TABLE

REAGENT or RESOURCE	SOURCE	IDENTIFIER
Biological samples		
Fossil *Nomgoliella sinistrivolubilis* specimens	Swedish Museum of Natural History	N/A
Thin section specimens	Ocean University of China	N/A
Deposited data		
RAW Raman data	This study	N/A
Measurement of shell tubules	This study	Table S1
Software and algorithms		
CorelDraw X9	Bouton, 2008[77]	https://www.coreldraw.com/cn/
Adobe Photoshop CC	Press, 2010[78]	https://www.adobe.com/
ImageJ 1.8.0	Burger and Burge, 2006[79]	https://imagej.nih.gov/ij/
Microsoft Excel	Microsoft Corporation	https://www.microsoft.com/en-us/microsoft-365/microsoft-office

RESOURCE AVAILABILITY

Lead contact

Further information and requests for resources and reagents should be directed to and will be fulfilled by the lead contact, Xingliang Zhang (xzhang69@nwu.edu.cn).

Materials availability

- Phosphatic internal mould specimens and thin sections of *Nomgoliella sinistrivolubilis* studied in this paper are deposited at the Department of Palaeobiology, Swedish Museum of Natural History (SMNH), and the College of Marine Geoscience, Ocean University of China (OUC), respectively.
- This study did not generate new unique reagents.

Data and code availability

- All relevant data is available in the main text and the Table S1.
- This paper does not report original code.
- Any additional information required to reanalyze the data reported in this paper is available from the lead contact upon request.

EXPERIMENTAL MODEL AND STUDY PARTICIPANT DETAILS

The experimental model and subject of this study only includes fossil specimens.

METHOD DETAILS

Material and sample preparation

The rock samples were broken and macerated in diluted 5% acetic acid solution to retrieve three-dimensional (3D) skeletal fossils at the Department of Palaeobiology, Swedish Museum of Natural History. Samples were left in acid for a week and the acid-resistant residues were washed, wet-sieved carefully through 60 μm sieves, and air-dried at room temperature. Abundant phosphatized mollusk specimens together with other skeletal fossils were manually picked under stereomicroscopy. *Nomgoliella sinistrivolubilis* was very common in the molluskan assemblage of the Bayangol Formation of southwestern Mongolia, and hundreds of specimens have been collected from the acid-resistant residues after acid treatment.

Electron microscopy

Scanning Electron Microscopy (SEM) and Backscattered electron (BSE) imaging were used to examine the morphological characters and fine details of preserved shell tubules on the surface of phosphatic internal moulds. Selected specimens were mounted on stubs, sputter-coated with golds, and examined with an FEI Quanta FEG 650 SEM at an accelerating voltage of 15 KV and 10–15 mm working distances in secondary

electron mode at the Department of Palaeobiology, Swedish Museum of Natural History. Backscattered electron imaging was obtained with an FEI Quanta FEG 650 SEM at an accelerating voltage of 10 KV and 10–15 mm working distances.

Optical microscopy

Nomgoliella sinistrivolubilis and other molluskan taxa were most abundant and diversified in the top horizon of the section. A rock sample collected from the 341m bed layer was cut to make petrographic thin sections (30 μm in thickness) at the Department of Geology, Northwest University. Thin sections parallel to pore-canal tubules of mineralized shells were observed through a Nikon LV100POL microscope equipped with a digital camera.

Confocal laser scanning microscopy

Confocal laser scanning fluorescence (CLSF) imaging was performed on a Zeiss LSM 900 confocal microscope equipped with an Airyscan 2 detector and a Zeiss ×50 objective. Fluorescence excitation was achieved by a 488nm diode laser. Experiment was conducted at the Shaanxi Key Laboratory of Early Life and Environments (LELE), and the State Key Laboratory of Continental Dynamics at the Northwest University (NWU).

Raman spectroscopy

Raman spectra (RS) for mineral detection were carried out on the clear surfaces of thin sections by use of a Horiba LabRAM Odyssey Raman spectrometer under a ×50 objective. A 532 nm laser with a 10% ND filter was selected for Raman excitation. Raman images of apatite, calcite, and kerogen were acquired in the spectral window of 955–975 cm^{-1}, 1077–1097 cm^{-1}, and 1200–1680 cm^{-1}, respectively. Experiment was conducted at the Shaanxi Key Laboratory of Early Life and Environments (LELE), and the State Key Laboratory of Continental Dynamics at the Northwest University (NWU). All images were processed in Adobe Photoshop CC[77] and CorelDraw X9.[78]

QUANTIFICATION AND STATISTICAL ANALYSIS

Measurements and calculations of the distribution and density of tubules within shells were performed on high-resolution SEM and BSE images by using ImageJ software.[79] Because the shell tubule was substituted by phosphate minerals and retained on the surface of internal moulds, it is possible that some tubules were missing or have not been preserved, thus specimens were carefully scrutinized (five most well preserved specimens were selected) to measure the tubular density of shells. To minimize errors, tubular density (N/mm^2) and diameter (D/μm) were measured at an average of five localities on each specimen with area of each square grid G = 0.5 mm × 0.5 mm = 0.25 mm^2. The area (A) of individual tubule was calculated as: $A = \pi \times (D/2)^2$, and thus the percentage (P) of shell tubules accounting for the entire shell volume was further calculated as follows: $P = A \times 10^{-6} \times N/G$, with average value P (average) = 34.98%. All mathematical calculation was performed in Microsoft Excel.